OPTIMAL DESIGN OF DAMPED DYNAMIC VIBRATION ABSORBER FOR DAMPED PRIMARY SYSTEMS

Kefu Liu, Gianmarc Coppola
Department of Mechanical Engineering, Lakehead University, 955 Oliver Rd. Thunder Bay, Ontario, Canada
E-mail: kliu@lakeheadu.ca

Received July 2009, Accepted February 2010
No. 09-CSME-38, E.I.C. Accession 3124

ABSTRACT

This study focuses on the optimum design of the damped dynamic vibration absorber (DVA) for damped primary systems. Different from the conventional way, the DVA damper is connected between the absorber mass and the ground. Two numerical approaches are employed. The first approach solves a set of nonlinear equations established by the Chebyshev's equioscillation theorem. The second approach minimizes a compound objective subject to a set of the constraints. First the two methods are applied to classical systems and the results are compared with those from the analytical solutions. Then the modified Chebyshev's equioscillation theorem method is applied to find the optimum damped DVAs for the damped primary system. Various results are obtained and analyzed.

CONCEPTION OPTIMALE D'UN AMORTISSEUR DYNAMIQUE DE VIBRATIONS POUR UN SYSTÈME PRIMAIRE D'AMORTISSEMENT

RÉSUMÉ

L'étude met l'accent sur la conception optimale d'un amortisseur dynamique de vibrations (ADV) pour un système primaire d'amortissement. Différent de la méthode conventionnelle, l'amortisseur ADV est connecté entre la masse-ressort et le sol. Deux approches numériques sont utilisées. La première approche résout un ensemble d'équations non-linéaires établies par le théorème d'équioscillation de Chebyshev. La deuxième approche minimise un objectif composé soumis à un ensemble de contraintes. Dans un premier temps, les deux méthodes sont appliquées à des systèmes classiques, et les résultats sont comparés avec ceux issus des solutions analytiques. Ensuite la méthode du théorème d'équioscillation de Chebyshev modifié est appliquée pour trouver l'amortissement optimal ADV pour un système primaire d'amortissement. Des résultats variés ont été obtenus et analysés.

1. INTRODUCTION

The dynamic vibration absorber (DVA) or tuned-mass damper (TMD) is a widely used passive vibration control device. When a mass-spring system, referred to as primary system, is subjected to a harmonic excitation at a constant frequency, its steady-state response can be suppressed by attaching a secondary mass-spring system or DVA. This idea was pioneered by Watts [1] in 1883 and Frahm [2] in 1909. However, a DVA consisting of only a mass and spring has a narrow operation region and its performance deteriorates significantly when the exciting frequency varies. The performance robustness can be improved by using a damped DVA that consists of a mass, spring, and damper. The key design parameters of a damped DVA are its tuning parameter and damping ratio. The first mathematical theory on the damped DVA was presented by Ormondroyd and Den Hartog [3]. Since then, many efforts have been made to seek optimum parameters for the damped DVA. In [4], Den Hartog first tackled the optimum solution of a damped DVA that is attached to a classical primary system, i.e., a system free of damping. His study utilized the feature of "fixed-point" frequencies, i.e., frequencies at which the response amplitude of the primary mass is independent of the absorber damping. Based on the "fixed-points" theory, Den Hartog found the optimum tuning parameter and defined the optimality for the optimum absorber damping. Based on this optimality, Brock [5] derived an analytical solution for the optimum damping ratio of the damped DVA.

A real system possesses a certain degree of damping. Figure 1 shows a damped primary system attached by a damped DVA. In the figure, m, c, and k denote mass, damping value, and stiffness of the primary system, respectively and m_a, c_a, and k_a mass, damping value, and stiffness of the absorber system, respectively. When a primary system is damped, the useful "fixed-points" feature is lost. Thus, obtaining a closed-form solution for the optimum tuning parameter or optimum damping ratio becomes impossible. A number of studies have focused on the numerical solutions. These include a numerical optimization scheme proposed by Randall *et al.* [6], an optimal design of linear and non-linear vibration absorbers using nonlinear programming techniques by Soom [7], and an optimum design using a frequency locus method by Thompson [8]. Notably, Pennestri [9] used the min-max Chebyshev's criterion to seek the optimum solutions. It was claimed that the method guarantees the uniqueness of the optimal solution (a question overlooked by many authors). Recently Ghosh and Basu [10] derived an approximate analytical solution for the optimum tuning parameter based on the assumption

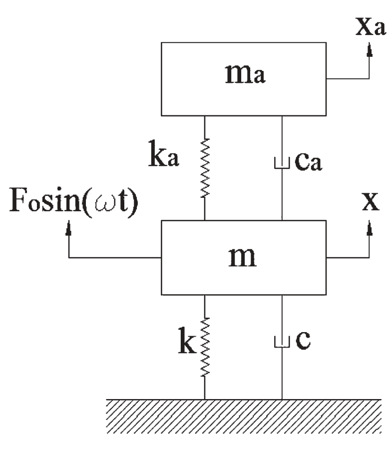

Fig. 1. Model A.

that the "fixed-points" theory also approximately holds when a damped DVA is attached to a lightly or moderately damped primary system.

Figure 2 shows a different way to attach a damper to the absorber mass. In this study, the damped DVA in Fig. 1 is referred to as Model *A* while the damped DVA in Fig. 2 is referred to as Model *B*. In [11], we presented the analytical solutions for the optimum parameters of Model *B* attached to a classical primary system. Although Model *B* is not as common as Model *A*, it does provide a viable alternative for some applications. For example, in [11], we showed that Model *B* outperforms Model *A* in terms of overall vibration suppression. In [12], Wong and Cheung derived the formulae for the optimum parameters for the case where Model *B* is attached to a structure excited by ground motion. They also showed that Model *B* provides a greater vibration suppression than Model *A*. Sometimes, a damper is too massive to be attached between the primary mass and the absorber mass. In such a case, Model *B* offers a solution. In [13], we utilized Model *B* to realize a damped DVA whose damping ratio can be tuned on-line. Another potential application is to use Model *B* to achieve two goals: vibration suppression and energy harvesting. The work reported in [14] investigated vibration confinement and energy harvesting in flexible structures using vibration absorbers and piezoelectric devices. Two possible configurations were considered for the installation of piezoelectric devices: either embedded between the structure and the absorber mass or between the ground and absorber mass. They found that the second configuration yields faster extraction of vibration energy.

It is noted that no results have been reported on the optimum parameters of Model *B* when it is attached to a damped primary system. This study intends to address this problem. First we derive an approximate closed-form solution for the optimum tuning parameter for the case where Model *B* is attached to a lightly or moderately damped primary system. Then, we tackle the problem in two different numerical ways. In the first way, we solve the problem using the Chebyshev's equioscillation theorem employed in [9]. In the second way, we formulate it as a constrained optimization problem and solve it by using the Nelder-Mead or sequential simplex method [15]. The numerical methods are first applied to both Model *A* and Model *B* attached to the classical primary system. The results are compared with those from the analytical solutions. Then the study focuses on Model *B* attached to the damped primary system. Various results are obtained and discussed.

The rest of the paper is organized as follows. In Section two, the mathematical models are presented and the analytical solutions for the classic primary system are given. In Section three,

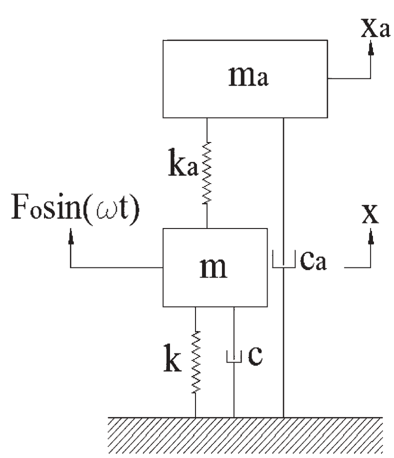

Fig. 2. Model B.

an approximate closed-form solution for the optimum tuning parameter is derived. In Section four, the numerical solution methods are explained. In Section five, the numerical solution results are given and the discussions are presented. In Section six, the conclusions of the study are drawn.

2. MODELS

Model A. The equation of motion for Model A is given by

$$\begin{bmatrix} m & 0 \\ 0 & m_a \end{bmatrix}\begin{bmatrix} \ddot{x} \\ \ddot{x}_a \end{bmatrix}+\begin{bmatrix} c+c_a & -c_a \\ -c_a & c_a \end{bmatrix}\begin{bmatrix} \dot{x} \\ \dot{x}_a \end{bmatrix}+\begin{bmatrix} k+k_a & -k_a \\ -k_a & k_a \end{bmatrix}\begin{bmatrix} x \\ x_a \end{bmatrix}=\begin{bmatrix} F_0 \\ o \end{bmatrix}\sin(\omega t) \tag{1}$$

where m, k, and c are the mass, stiffness, and damping value of the primary system, respectively, m_a, k_a, and c_a are the mass, stiffness, and damping value of the absorber system, respectively, F_0 and ω are the amplitude and frequency of the exciting force, respectively, x and x_a are the displacement of the primary mass and the absorber mass, respectively. The normalized amplitude of the steady-state response of the primary mass is given as:

$$G=\left|\frac{X}{Fo/k}\right| = \sqrt{\frac{\left(1-\frac{r^2}{\beta^2}\right)^2+4\left(\zeta_a\frac{r}{\beta}\right)^2}{\left(\frac{r^4}{\beta^2}-(\frac{4\zeta_a\zeta_p}{\beta}+\frac{1}{\beta^2}+(\mu+1))r^2+1\right)^2+4\left(r\left(\zeta_p+\frac{\zeta_a}{\beta}\right)-\frac{r^3}{\beta}\left(\zeta_a+\frac{\zeta_p}{\beta}\right)-\frac{r^3}{\beta}\zeta_a\mu\right)^2}} \tag{2}$$

where $\omega_p=\sqrt{\frac{k}{m}}$, $\zeta_p=\frac{c}{2m\omega_p}$, $\omega_a=\sqrt{\frac{k_a}{m_a}}$, $\zeta_a=\frac{c_a}{2m_a\omega_a}$, $\beta=\frac{\omega_a}{\omega_p}$, $\mu=\frac{m_a}{m}$, $r=\frac{\omega}{\omega_p}$.

For the classical system, i.e., $\zeta_p = 0$ [5], the optimum tuning parameter is given by

$$\beta^*=\frac{1}{1+\mu} \tag{3}$$

and the optimum damping ratio for the absorber is given by

$$\zeta_a^*=\sqrt{\frac{3\mu}{8(1+\mu)}} \tag{4}$$

Model B. The equation of motion for Model B is given by:

$$\begin{bmatrix} m & 0 \\ 0 & m_a \end{bmatrix}\begin{bmatrix} \ddot{x} \\ \ddot{x}_a \end{bmatrix}+\begin{bmatrix} c & 0 \\ 0 & c_a \end{bmatrix}\begin{bmatrix} \dot{x} \\ \dot{x}_a \end{bmatrix}+\begin{bmatrix} k+k_a & -k_a \\ -k_a & k_a \end{bmatrix}\begin{bmatrix} x \\ x_a \end{bmatrix}=\begin{bmatrix} F_0 \\ o \end{bmatrix}\sin(\omega t) \tag{5}$$

The normalized amplitude of the steady-state response of the primary mass is given as:

$$G=\left|\frac{X}{Fo/k}\right|$$

$$=\sqrt{\frac{\left(1-\frac{r^2}{\beta^2}\right)^2+4\left(\zeta_a\frac{r}{\beta}\right)^2}{\left(\frac{r^4}{\beta^2}-(\frac{4\zeta_a\zeta_p}{\beta}+\frac{1}{\beta^2}+(\mu+1))r^2+1\right)^2+4\left(r\left(\zeta_p+\frac{\zeta_a}{\beta}\right)-\frac{r^3}{\beta}\left(\zeta_a+\frac{\zeta_p}{\beta}\right)+r\beta\zeta_a\mu\right)^2}} \tag{6}$$

For the classical system, i.e., $\zeta_p = 0$ [11], the optimum tuning parameter is given by

$$\beta^*=\frac{1}{\sqrt{1-\mu}} \tag{7}$$

and the optimum damping ratio for the absorber is given by

$$\zeta_a^*=\frac{1}{2}\sqrt{\frac{3\mu}{2-\mu}} \tag{8}$$

3. APPROXIMATE ANALYTICAL OPTIMUM TUNING PARAMETER

To understand Den Hartog's optimality for the damped DVA, we show Fig. 3 which compares the normalized amplitudes of the primary mass when Model *A* is attached to a classical primary system, i.e., $\zeta_p = 0$. The mass ratio is μ =0.1 and the tuning parameter is optimum, i.e., $\beta^* = 1/$

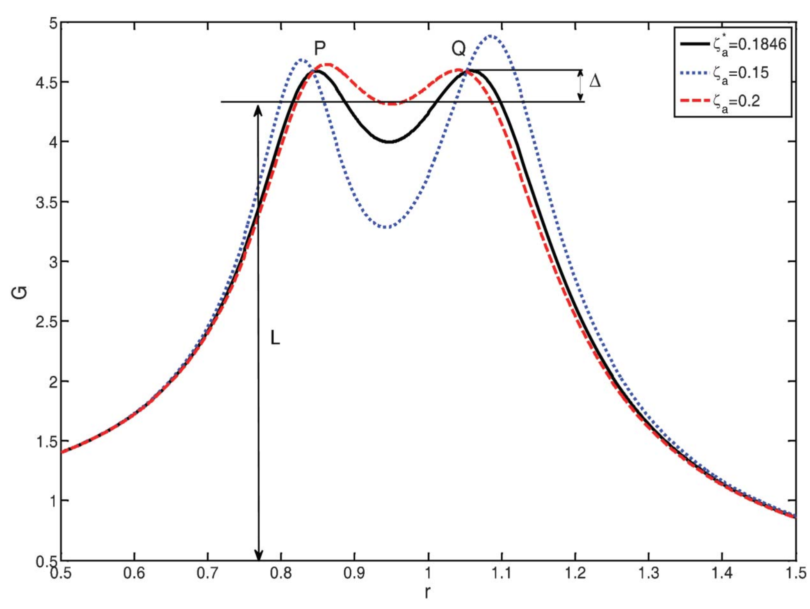

Fig. 3. Normalized amplitudes of the primary mass attached by model *A* with μ =0.1 and β*.

(1+μ). It can be seen that the three curves join at two common points P and Q, i.e., fixed-points. As predicted by Den Hartog's optimality, the use of the optimum tuning parameter β* ensures that $G_P = G_Q$ regardless of the damping levels of the damped DVA. The solid line represents the damped DVA with the optimum damping ratio ζ_a^*. This optimum damping ratio makes the curve slope at points P and Q almost zero, i.e., $G_{\max} \approx G_P \approx G_Q$.

When a primary system is damped, the ‘‘fixed-points’’ feature no longer exists. However, as shown in [10], when a damped DVA with a small mass ratio is attached to lightly or moderately damped primary systems, the normalized amplitude curves roughly join at two points. When the primary system damping ratio approaches zero, these two points converge to the ‘‘fixed-points P and Q, respectively. We observe the same patterns for the damped primary system attached by Model B. Therefore it is justified to assume that the ‘‘fixed-point’’ theory also approximately holds even for the case when a damped DVA is attached to a lightly or moderately damped primary system. Based on this assumption, we derive an approximate solution for the optimum tuning parameter for the damped Model B. To this end, we rearrange Eq. (6) in the following form:

$$G=\sqrt{\frac{A\zeta_a^2+B}{C\zeta_a^2+D\zeta_a+E}} \tag{9}$$

where

$$A=4\frac{r^2}{\beta^2},\ B=\left(1-\frac{r^2}{\beta^2}\right)^2,\ C=\frac{16\zeta_p^2r^4}{\beta^2}+4\left(\frac{r}{\beta}+\beta r\mu-\frac{r^3}{\beta}\right)^2$$

$$D=-\frac{8\left(\frac{r^4}{\beta^2}-\frac{r^2}{\beta^2}-r^2(\mu+1)+1\right)\zeta_p r^2}{\beta}+16\left(\zeta_p r-\frac{\zeta_p r^3}{\beta^2}\right)\left(\frac{r}{\beta}+\beta r\mu-\frac{r^3}{\beta}\right)$$

$$E=\left(\frac{r^4}{\beta^2}-\frac{r^2}{\beta^2}-r^2(\mu+1)+1\right)^2+4\left(\zeta_p r-\frac{\zeta_p r^3}{\beta^2}\right)^2$$

According to the ‘‘fixed-point’’ theory assumption, there exist two invariant points on the G verses r curve where G is independent of ζ_a. To find these points, let ζ_a=0, we have $G=\sqrt{B/E}$ and let $\zeta_a\to\infty$, we have $G=\sqrt{A/C}$. Equating them results in

$$\frac{\left(1-\frac{r^2}{\beta^2}\right)^2}{\left(\frac{r^4}{\beta^2}-\frac{r^2}{\beta^2}-r^2(\mu+1)+1\right)^2+4\left(\zeta_p r-\frac{\zeta_p r^3}{\beta^2}\right)^2}=\frac{\frac{4r^2}{\beta^2}}{\frac{16\zeta_p^2r^2}{\beta^2}+4\left(\frac{r}{\beta}+\beta r\mu-\frac{r^3}{\beta}\right)^2} \tag{10}$$

This expression can then be solved for the frequency ratios corresponding to the fixed points

$$r_{P,Q} = \sqrt{\frac{1+(1+\mu)\beta^2 \mp \sqrt{1+2(\mu-1)\beta^2+(\mu^2+1)\beta^4}}{2}} \tag{11}$$

Not supprisingly, the solutions are the same as those given in Eq. (8) of [11]. It is interesting to note that the two fixed frequency ratios are independent of ζ_p. The ordinates of points P and Q can be found by letting $\zeta_a \to \infty$ in Eq. (9)

$$G = \sqrt{\frac{A}{C}} = \sqrt{\frac{1}{4\zeta_p^2 r^2 + \left(1+\beta^2\mu - r^2\right)^2}} \tag{12}$$

Abiding by our assumption that the normalized amplitude at the points P and Q must be equal, we equate $G_B(r_P)$ to $G_B(r_Q)$

$$\frac{1}{4\zeta_P^2 r_P^2 + \left(1+\beta^2\mu - r_P^2\right)^2} = \frac{-1}{4\zeta_P^2 r_Q^2 + \left(1+\beta^2\mu - r_Q^2\right)^2} \tag{13}$$

which yeilds

$$\beta^* = \sqrt{\frac{1-4\zeta_p^2}{1-\mu}} \tag{14}$$

If $\zeta_p = 0$, the above equation is reduced to Eq. (7), i.e., the optimum tuning parameter for Model B attached to a classical primary system.

4. NUMERICAL SOLUTION METHODS

Refer to Fig. 3. According to the interpretation presented in [9], the most favourable curve has the same maximum normalized amplitudes or the curve can be best approximated by the line of $G = L$. Thus, the Chebyshev equioscillation theorem can be used to find the optimum values of β and ζ_a such that the function G has 2 equal peak values with a minimal distance from a straight line L. This way, the optimum solution can be obtained by solving the following 6 non-linear algebraic equations:

$$\left.\frac{dG}{dr}\right|_{r=r_1} = 0, \left.\frac{dG}{dr}\right|_{r=r_2} = 0, \left.\frac{dG}{dr}\right|_{r=r_3} = 0, \tag{15a–c}$$

$$G(r_1) - G(r_3) = 0,\ 2L - (G(r_2) + G(r_3)) = 0,\ 2\Delta - (G(r_1) - G(r_2)) = 0 \tag{15d–f}$$

where Δ is the maximum deviation of the response curve from the value $G = L$ and r_1, r_2, and r_3 are the frequency ratios where the curves reaches a maximum or minimum. As there are only 6

equations for 7 unknowns (i.e., ζ_a, β, L, $\Delta\, r_1$, r_2, and r_3), the solutions must be conducted by prescribing a value for one of the 7 unknowns. In [9], the equations were solved using a numerical solver for non-linear equations for different prescribed values of ζ_a and the chosen solution set was the one with the minimum value of $G_{\max}$.

The problem can also be formulated as the one that minimizes the following two functions

$$f_1(\beta,\zeta_a)=|G(r_3)-G(r_1)| \tag{16a}$$

$$f_2(\beta,\zeta_a)=G_{\max} \tag{16b}$$

An objective function can be defined as

$$f(\beta,\zeta_a)=w_1 f_1(\beta,\zeta_a)+w_2 f_2(\beta,\zeta_a) \tag{17}$$

where w_1 and w_2 are weighting factors used to impose different emphasis on each of the functions. The optimum solution can be found by solving the following constrained optimization problem:

Minimize $f(\beta,\zeta_a)$
subject to $\beta_{low}\leq\beta\leq\beta_{up}$, $\zeta_{alow}\leq\zeta_a\leq\zeta_{aup}$ ensuring the existence of $G(r_1)$, $G(r_2)$, and $G(r_3)$. (18)

where β_{low} and β_{up} are the lower bound and upper bound for β, respectively, and ζ_{alow} and ζ_{up} are the lower bound and upper bound for ζ_a, respectively.

5. RESULTS AND DISCUSSION

The nonlinear Eqs. (15a–f) were solved using the fsolve function provided in Matlab's Optimization toolbox. The fsolve function requires providing a set of initial values for the parameters. It is noted that the proper selection of the initial parameter set is critical to the convergence of the fsolve function. In the solution, the optimum results from solving the optimization problem of Eq. (18) were used as initial parameters for the fsolve function. The optimization problem of Eq. (18) was solved using the sequential simplex or the Nelder-Mead algorithm programmed in Matlab. The bounds for the parameters were set as: $\beta_{low} = 0$, $\beta_{high} = 2$ and $\zeta_{alow} = 0$, $\zeta_{ahigh} = 0.85$. Understandably, a solution to the optimization problem of Eq. (18) depends on the weighting factor values used in the objective function and an initial simplex provided to the sequential simplex algorithm. In each solution, an initial simplex was randomly generated within the feasible region. After some trial and error tests, the weights used in Eq. (17) were chosen to be $w_1 = 0.1$ and $w_2 = 1$.

5.1 Results of the Models Attached to a Classical Primary System

First we apply the solution methods to the classical system, i.e., $\zeta_p = 0$. For brevity, the following acronyms are defined: NM for the Nelder-Mead or sequential simplex method, CH for Chebyshev's theorem, and AN for the analytical method. The results for Model *A* are given in Figs. 4 and 5 and Table 1. It can be seen that the results from the two numerical methods are quite close to those obtained by the analytical method.

The results for Model *B* are presented in Figs. 6, 7, 8 and Table 2. For small mass ratios such as μ =0.05 or 0.1, the numerical results are very close to the analytical ones. When the mass

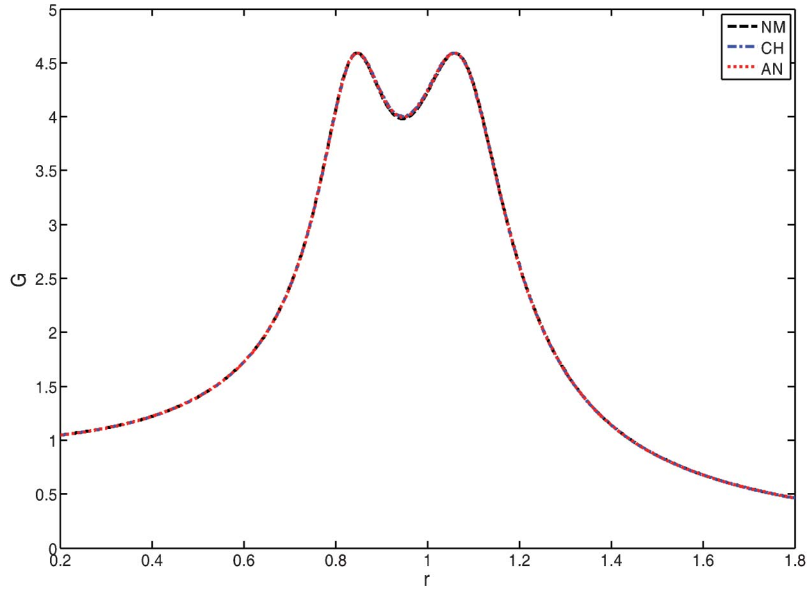

Fig. 4. Normalized amplitudes with the optimum Model A when $\mu = 0.1$.

ratio increases, the discrepancy between the numerical results and the analytical ones increases. It is also noted that when $\mu > 0.2$, the NM results differ significantly from the CH results. Figure 7 explains what causes such a disagreement. When the mass ratio is large, the CH solution tends to converge to a response curve that has a single peak. This corresponds to the case of $r_1 = r_2 = r_3$ which is a valid solution to Eqs. (15a–f). The other possible solutions to Eqs. (15a–f) are $r_1 = r_2$ or $r_2 = r_3$. Because the use of the fsolve function to solve the nonlinear Eqs. (15a–f) is an unconstrained optimization problem, it cannot guarantee the existence of distinct $G(r_1)$, $G(r_2)$, and $G(r_3)$. In this case, the NM and CH solutions are no longer comparable. In

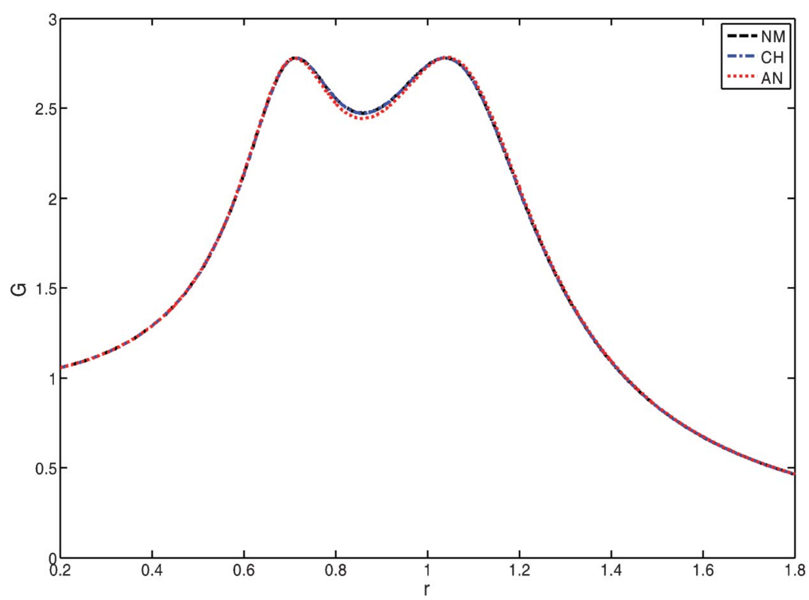

Fig. 5. Normalized amplitudes with the optimum Model A when $\mu = 0.3$.

Table 1. Optimum results for Model *A* attached to a classical primary system.

	β			ζa		
μ	NM	CH	AN	NM	CH	AN
0.05	0.95243	0.9524	0.95238	0.13309	0.13355	0.13363
0.1	0.90919	0.9091	0.90909	0.18396	0.18498	0.18464
0.15	0.8696	0.86948	0.86057	0.22165	0.22282	0.22116
0.2	0.83314	0.83319	0.83333	0.25298	0.25249	0.25
0.25	0.79979	0.79986	0.8	0.27726	0.27663	0.27386
0.3	0.76897	0.76898	0.76923	0.29838	0.29819	0.29417

order to overcome this problem, we modified the CH method by imposing two additional conditions: $r_1 > r_2$ and $r_2 < r_3$. The dash-dotted line on Fig. 7 was obtained using the modified CH method. Now the NM and modified CH solutions are almost overlapping one another.

Table 3 compares the performances achieved by the optimum DVAs in terms of the maximum normalized amplitudes. The difference between the numerical solutions and the analytical solution requires an explanation. It is noted that with a larger μ, the numerical solutions tend to result in a larger β and a larger ζ_a, which makes the response curve flatter. In using the fixed-points theory to derive the analytical solution, first the condition of $G_P = G_Q$ is enforced to obtain the optimum tuning parameter β^* and then the optimum damping ratio ζ_a^* is found by fixing β^*. However, the numerical solutions assume that β and ζ_a can be varied arbitrarily within the given bounds. Rigorously speaking, the results with different β values are not comparable. If we set β^* as the upper bound for β, then the three methods give a similar result as shown in Fig. 8. From a dynamics viewpoint, for Model *B*, a DVA with a larger β facilitates the energy dissipation because the damping force is proportional to the absolute

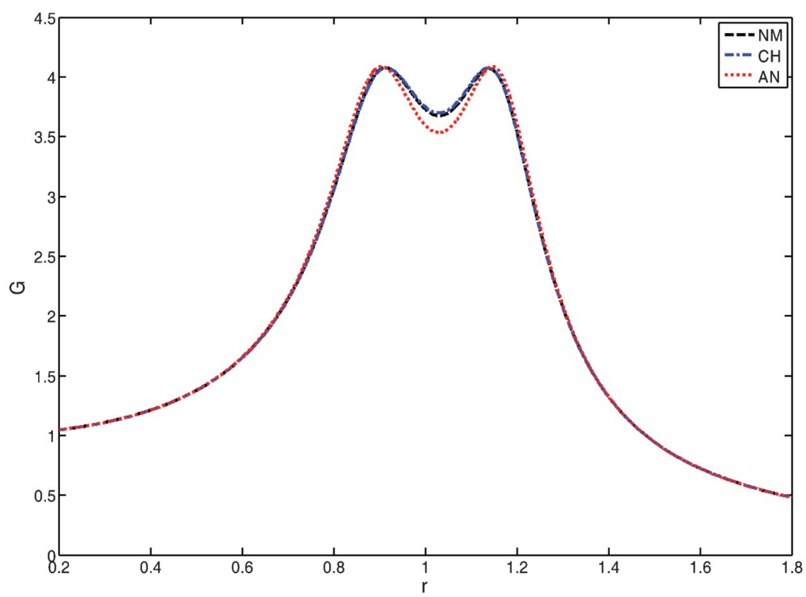

Fig. 6. Normalized amplitudes with the optimum Model *B* when $\mu = 0.1$: NM (dashed line), CH (dash-dot line), AN (dotted line).

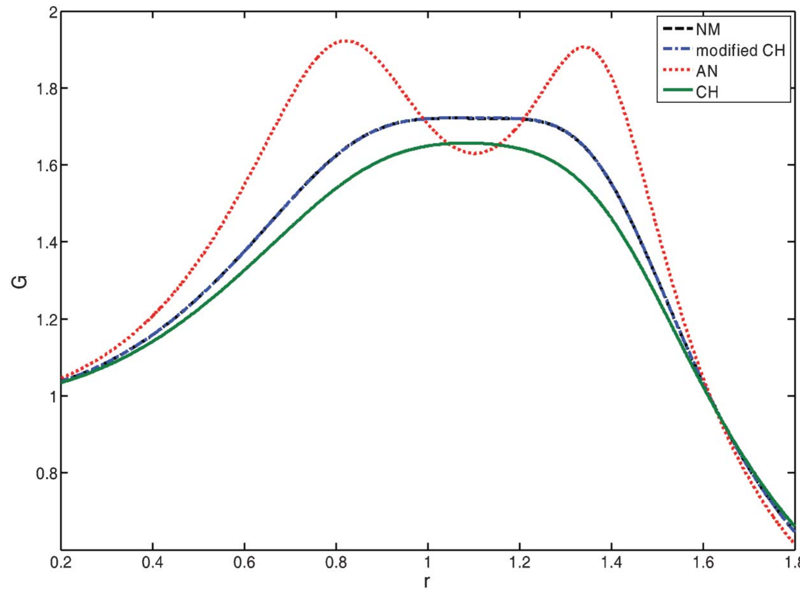

Fig. 7. Normalized amplitudes with the optimum Model *B* when $\mu = 0.3$.

displacement of the absorber mass. This is not the case for Model *A* because its damping force is proportional to the relative displacement of the absorber mass.

5.2 Results of Model *B* Attached to a Damped Primary System

In the following, we report only the results using the modified Chebyshev's method. We considered $0.05 \leq \mu \leq 0.25$ and $0 \leq \zeta_p \leq 0.4$. Figures 9(a) and (b) show the computed optimum values for the tuning parameter corresponding to four mass ratios. In the figures, we also show the analytical results computed using the approximate solution of Eq. (14). From these results,

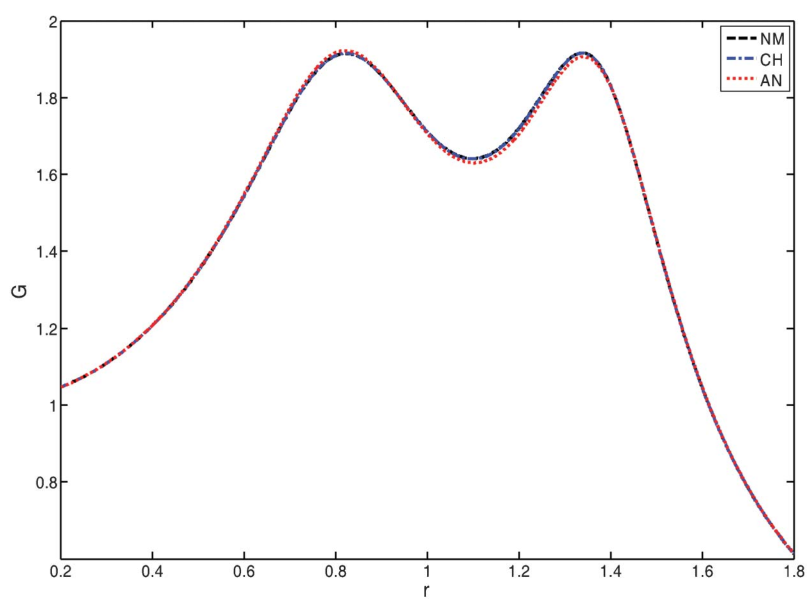

Fig. 8. Normalized amplitudes when $\mu = 0.3$ and $\beta = \beta^* = 1/(1+\mu)$.

Table 2. Comparison of the results for the optimum Model *B*.

	β			ζa		
μ	NM	CH	AN	NM	CH	AN
0.05	1.0266	1.0268	1.026	0.14153	0.14223	0.13868
0.1	1.0577	1.0579	1.0541	0.20817	0.20954	0.19868
0.15	1.0963	1.0962	1.0847	0.2709	0.27022	0.2466
0.2	1.1458	1.1475	1.118	0.33333	0.33567	0.28868
0.25	1.244	1.3858	1.1547	0.42539	0.50931	0.32733
0.3	1.2862	1.4329	1.1952	0.45522	0.54618	0.3638

one can note a few important attributes. Firstly, for a given ζ_p the optimal β value increases with an increase of μ. This trend differs from the one demonstrated in Model *A* [9]. For a given primary system, a DVA with a larger μ and larger β corresponds to a more massive and stiffer absorber system. Such a system enhances the energy dissipation in Model *B* and hinders the energy dissipation in Model *A*. The approximate solutions of Eq. (14) are close to the numerical solutions only when μ and ζ_p are small while both of the solutions follow a similar trend. This is expected as the approximate solution is derived based on the assumption of the existence of the "fixed-points" feature. Such an assumption is justified only for a system consisting of a lightly or moderately damped primary system and a DVA with a small mass ratio.

Figure 10 gives the relationships of ζ_a vs. ζ_p for four mass ratios. The trend in the optimum ζ_a values is similar for both the models, i.e. a larger μ value requires a larger ζ_a value and a larger ζ_p value demands a larger ζ_a value. However, the magnitude of the optimum ζ_a values for Model *B* is greater than that for Model *A* and the rate of increase in the optimum ζ_a with ζ_p for Model *B* is much faster than that for Model *A*.

Figures 11 and 12 show the normalized amplitudes of the primary mass vs. the frequency ratio. It is noted that increasing either ζ_p or μ makes the optimum response curve flatter. Figs. 13 and 14 show the maximum normalized amplitudes for the primary mass and the absorber mass, respectively. Both of the curves follow a general trend in which with an increase of the primary system damping the maximum amplitude of vibration is reduced. Also, with an increase of the mass ratio the maximum amplitude of vibration is reduced as well. This trend is similar to that of model *A* [9].

Table 3. Maximum normalized amplitudes of the primary mass (Gmax) and the absorber mass (Gamax) with the optimum Model *B*.

	Gmax			Ga max		
μ	NM	CH	AN	NM	CH	AN
0.05	6.0495	6.0487	6.0531	20.0304	19.8993	20.1589
0.1	4.0748	4.0744	4.0876	9.4106	9.4077	9.693
0.15	3.1522	3.1519	3.1796	5.8203	5.8381	6.1901
0.2	2.5646	2.5645	2.6186	3.982	3.9895	4.4346
0.25	2.1193	2.057	2.2228	2.7741	2.3525	3.3808
0.3	1.7233	1.6161	1.9222	1.9772	1.6345	2.6797

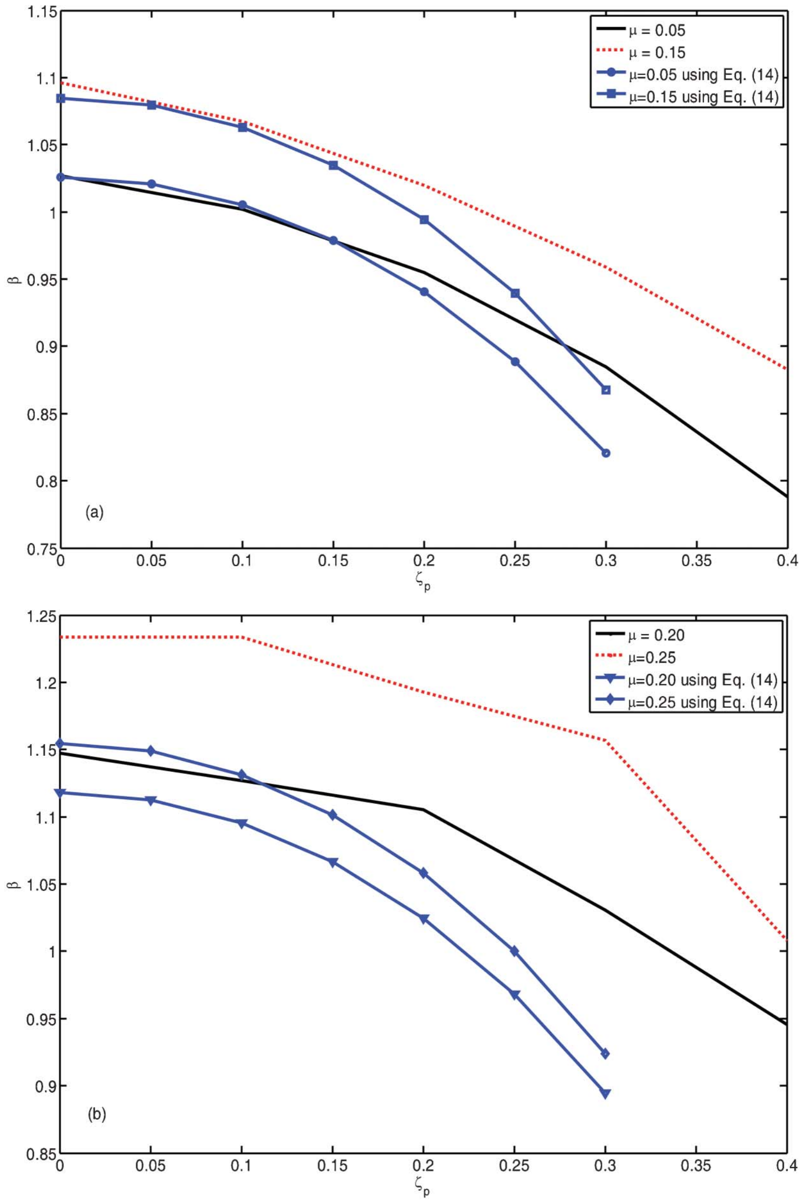

Fig. 9. Optimal tuning parameters, (a) $\mu = 0.05$ and $\mu = 0.15$; (b) $\mu = 0.20$ and $\mu = 0.25$.

Thus far, we have set $\mu_{\max} = 0.25$ as it is considered to be a practical upper bound [13]. Figure 12 reveals an interesting trend: with a large mass ratio, the greater the ζ_p values, the flatter the response curves. This provokes a question: what will happen if we increase μ further? Figure 15 shows the response curves with the optimum damped DVAs when $\mu = 0.35$. It is noted that the curves follow a different trend: the maximum normalized amplitude remains almost unchanged when the primary system damping increases. When the primary system damping is lower, the optimization results in a larger tuning parameter and a higher absorber system damping ratio.

The above study has shown that the optimum solution can be found by either solving the constrained optimization problem of Eq. (18) or solving Eqs. (15a–f). This leads us to question whether the problem can be reduced to solve only five Eqs. (15a–e) or four Eqs. (15a–d). The

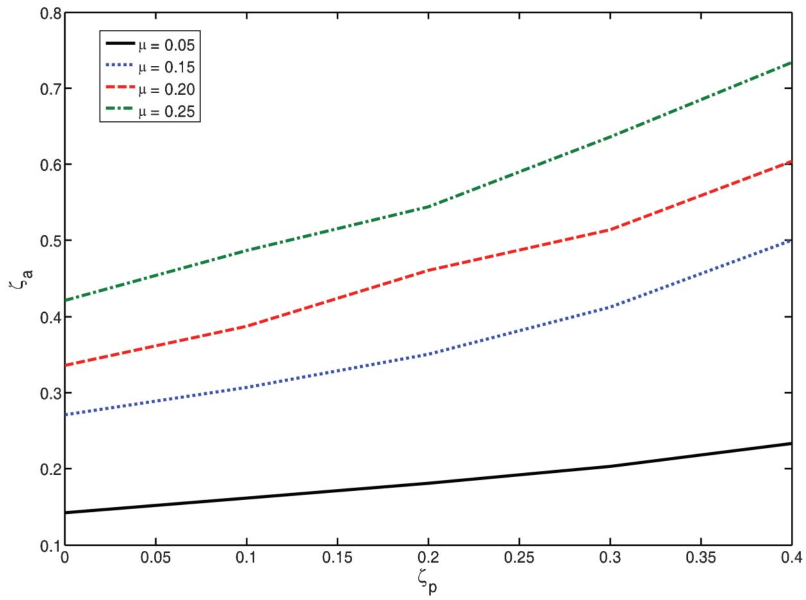

Fig. 10. Optimal damping ratios.

results have demonstrated that it is possible to do so. Due to the paper length, we omit the presentation of those results.

6. CONCLUSION

We have investigated the optimum design problem for a special damped dynamic vibration absorber referred to as Model *B*. First we derived an approximate closed-form solution for the optimum tuning parameter for the case where Model *B* is attached to a lightly or moderately damped primary system. Then, we tackled the problem using two different numerical methods.

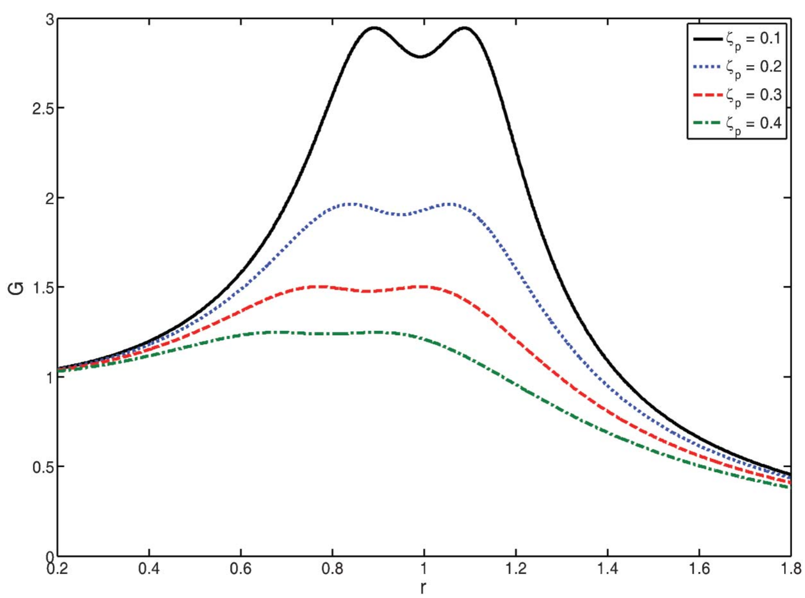

Fig. 11. Normalized amplitudes of the primary mass when $\mu = 0.05$.

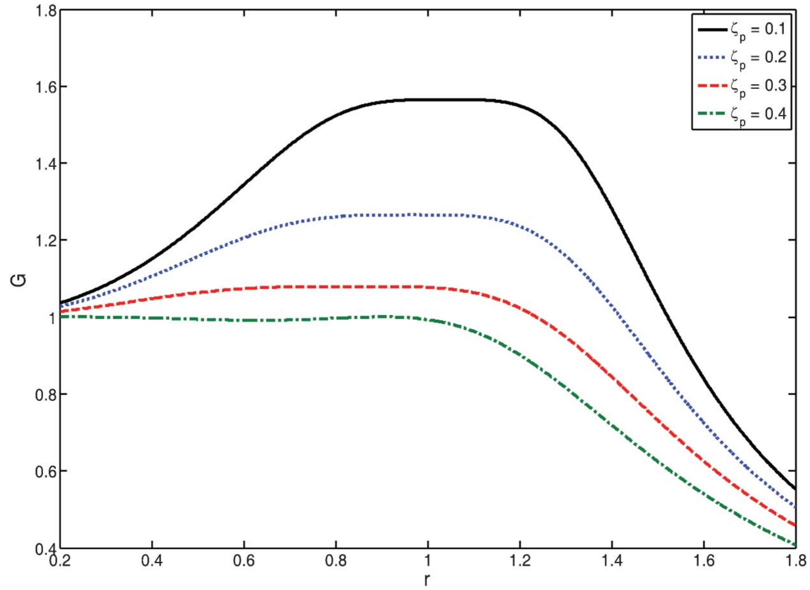

Fig. 12. Normalized amplitudes of the primary mass when $\mu = 0.25$.

The first method is based on the Chebyshev's equioscillation theorem. The second method formulates the problem as a constrained optimization problem that is solved using the sequential simplex algorithm. The numerical study contained two parts. The first part focused on a comparison of the analytical solutions and the numerical solutions for the cases where Model *A* or Model *B* is attached to a classical primary system. The study has shown that for Model *A*, a good agreement between the numerical results and analytical ones has been found whereas for Model *B*, the numerical results differ from the analytical ones when the mass ratio

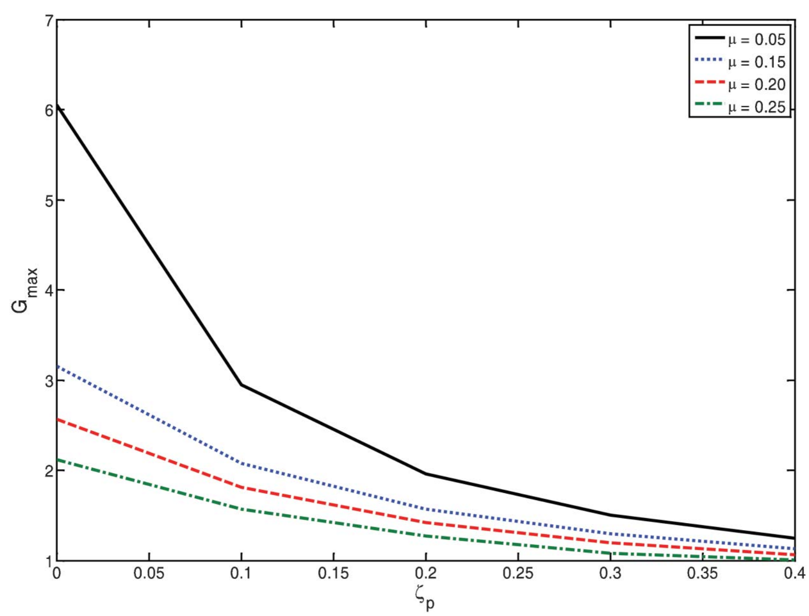

Fig. 13. The maximum normalized amplitudes of the primary mass: $\mu = 0.05$ (solid line), $\mu = 0.15$ (dotted line), $\mu = 0.20$ (dashed line), $\mu = 0.25$ (dash-dot line).

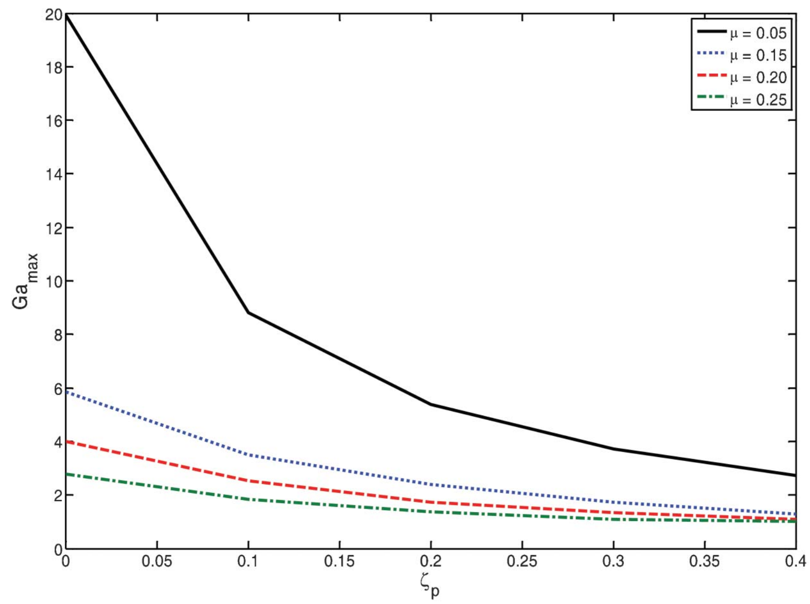

Fig. 14. The maximum normalized amplitudes of the absorber mass: $\mu = 0.05$ (solid line), $\mu = 0.15$ (dotted line), $\mu = 0.20$ (dashed line), $\mu = 0.25$ (dash-dot line).

increases. We have identified what causes a discrepancy between the numerical solutions and the analytical solutions for Model *B*. We have also revealed some possible incorrect convergences of the Chebyshev's method. To overcome this problem, we have modified the Chebyshev's method by imposing an additional selection criterion, i.e., existence of distinct $G(r_1)$, $G(r_2)$, and $G(r_3)$. In the second part, we have applied the modified Chebyshev's method to the case where Model *B* is attached to a damped primary system. The optimum values for the tuning parameter β and the damping ratio ζ_a have been found for various cases. It has been

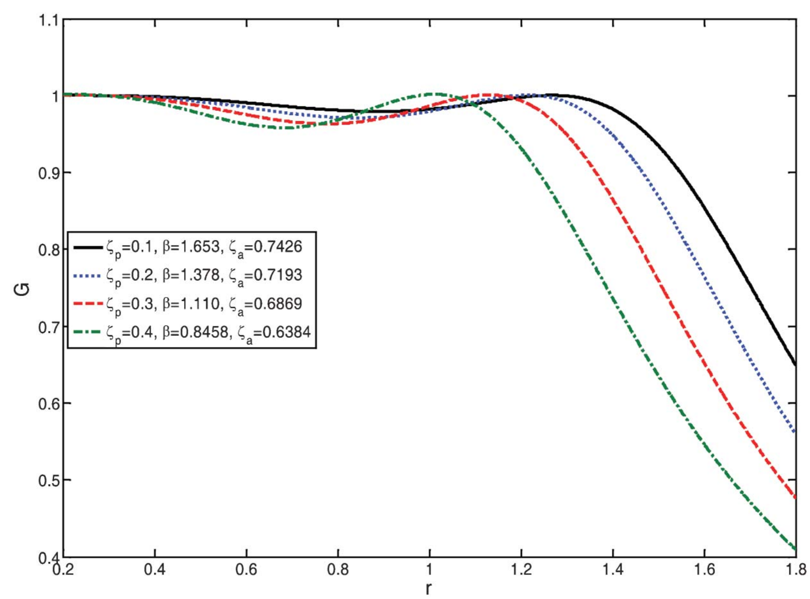

Fig. 15. Normalized amplitudes of the primary mass when $\mu = 0.35$.

found that with an increase of the damping ratio ζ_p or the mass ratio μ, the optimum tuning parameter β decreases and the optimum damping ratio ζ_a increases. The results have also revealed an interesting trend of the normalized amplitude of the primary mass when the mass ratio increases. Treating the problem as the constrained optimization, we have identified the limitations of the Chebysev's equioscillation theorem. We have shown that the proposed modified Chebysev's method are able to overcome such the limitations.

REFERENCES

1. Watts, P., ''On a method of reducing the rolling of ship at sea,'' *Transactions of the Institute of Naval Architects*, Vol. 24, pp. 165–190, 1883.
2. Frahm, H., ''Device for damping vibrations of bodies,'' U.S. Patent No. 989958, 1909.
3. Ormondroyd, J. and Den Hartog, J.P., ''Theory of the dynamic vibration absorber,'' *Transactions of the American Society of Mechanical Engineers*, Vol. 50, pp. 9–22, 1928.
4. Den Hartog, J.P., *Mechanical Vibrations*, McGraw-Hill, New York, 1934.
5. Brock, J. E., ''A note on the damped vibration absorber,'' *Journal of Applied Mechanics*, Vol. 68, pp. A-284, 1946.
6. Randall, S.E., Halsted D.M. and Taylor, D.L., ''Optimum vibration absorber for linear damped systems,'' *ASME Journal of Mechanical Design*, Vol. 103, pp. 908–913, 1981.
7. A. Soom, M.-S.L., ''Optimal design of linear and nonlinear vibration absorbers for damped systems,'' *ASME Journal of Vibration, Acoustics, Stress, and Reliability in Design*, Vol. 105, pp. 112–118, 1983.
8. Thompson, A.G., ''Optimizing the untuned viscous dynamic vibration absorber with primary system damping: a frequency locus method,'' *Journal of Sound and Vibration*, Vol. 77, pp. 469–472, 1980.
9. Pennestri, E., ''An application of Chebyshev's min-max criterion to the optimum design of a damped dynamic vibration absorber,'' *Journal of Sound and Vibration*, Vol. 217, pp. 757–765, 1998.
10. Ghosh, A. and Basu, B., ''A closed-form optimal tuning criterion for TMD in damped structures,'' *Structural Control and Health Monitoring*, Vol. 14, pp. 681–692, 2007.
11. Liu, K. and Liu, J., ''The damped dynamic vibration absorbers: revisited and new result,'' *Journal of Sound and Vibration*, Vol. 284, pp. 1181–1189, 2005.
12. Wong, W. and Cheung, Y., ''Optimal design of a damped dynamic vibration absorber for vibration control of structure excited by ground motion,'' *Engineering Structures*, Vol. 30, pp. 282–286, 2008.
13. Liu, K., Liu, J. and Liao, L., ''Application of a tunable electromagnetic damper in suppression of structural vibration,'' *Transactions of the Canadian Society for Mechanical Engineering*, Vol. 30, pp. 41–61, 2006.
14. Chtiba, M., Choura, S., Hayfeh, A. and El-Borgi, S., ''Vibration confinement and energy harvesting in flexible structures using collocated absorbers and piezoelectric devices,'' To appear in *Journal of Sound and Vibration*.
15. Belegundu, A. and Chandrupatla, T., *Optimization Concepts and Applications in Engieering*, Prentice-Hall, Inc., Upper Saddle River, New Jersey, 1999.
16. Inman, D. J., *Engineering Vibration*, 3rd Edition, Prentice-Hall, Inc., Upper Saddle River, New Jersey, 2008.